International Journal of Earth Sciences (2021) 110:35–51
https://doi.org/10.1007/s00531-020-01931-8

ORIGINAL PAPER

Deformation patterns and potential active movements of the Fansipan mountain range, northern Vietnam

Thi-Hue Dinh[1,2] · Yu-Chang Chan[1,2] · Chung-Pai Chang[3] · Chih-Tung Chen[4] · Yi-Chun Hsu[4]

Received: 24 December 2019 / Accepted: 3 September 2020 / Published online: 3 October 2020

Abstract

Located in northern Vietnam, the Fansipan mountain range is the highest topography in the Indochina area. Until recently, there has been limited research regarding the tectonic deformation of the Fansipan mountain range and whether there are notable surface ruptures or active faults in the area. This study provides the first insight into the deformation patterns and potential active movements of the Fansipan mountain range, and may improve our understanding of the overall tectonic activities in northern Vietnam. Our observations from ASTER 30-m DEM show a symmetrical mountain form in the north and an asymmetrical form in the south. The analysis of river profiles indicates similar patterns on both sides in the north and different patterns in the south with short and steep rivers on the SW side and long and gentle rivers on the NE side. The results of the normalized steepness index (k_{sn}) also show higher values on the SW side of the south part than the values from the other sides. These results suggest a spatial variation in rock uplift patterns of the Fansipan mountain range. Notably, the mountain front of the SW side of the southern Fansipan mountain range is associated with the Phong Tho-Nam Pia normal fault, suggesting that the normal faulting activity likely played an important role in tectonic uplift of this high mountain range. Our investigation of the stress field using fault kinematics indicates that the Fansipan mountain range and its surrounding areas are undergoing an inhomogeneous mixture of strike-slip and normal faulting. It is proposed that the strike-slip and normal motions alternated because of a permutation of σ_1/σ_2 under the same extensional stress regime of approximately NE–SW σ_3. This kinematic pattern may effectively control the recent tectonic movements in northern Vietnam.

Keywords Fansipan mountain range · River profile · Normalized steepness index (k_{sn}) · Stress field analysis · Active normal faulting · Stress permutation

Introduction

As a consequence of the collision between the India and Eurasian plates, many strike-slip faults and deformation structures developed in central and eastern Asia (Molnar and Tapponnier 1975; Tapponnier et al. 1982). Located in the southern part of the collisional deformation zone, northern Vietnam is considered among the most crucial regions for studying the tectonic evolution of SE Asia. The deformation structures of northern Vietnam are mainly characterized by several strike-slip faults (Fig. 1) including the Red River Fault (RRF) and the Dien Bien Phu Fault (DBPF). The RRF is an active right-lateral strike-slip fault with hundreds of kilometers in length, extending from southernmost China to northern Vietnam (Allen et al. 1984; Wang et al. 1998; Schoenbohm et al. 2004; Zuchiewicz et al. 2013). The DBPF is the most active strike-slip fault in northern Vietnam with large earthquakes greater than magnitude Mw 6.0 occuring in recorded history (Duong et al. 2013). Between these two active faults, the approximately 40 km wide, 150 km long Fansipan mountian range is topographically high region, comprising the highest mountian peak of 3143 m in the Indochina area (including Vietnam, Laos, and Cambodia). Although many

✉ Yu-Chang Chan
yuchang@earth.sinica.edu.tw

1 Taiwan International Graduate Program (TIGP) - Earth System Science Program, Academia Sinica and National Central University, Taipei, Taiwan

2 Institute of Earth Sciences, Academia Sinica, No. 128, Sec. 2, Academia Road, Taipei, Taiwan

3 Center for Space and Remote Sensing Research, National Central University, Zhongli, Taiwan

4 Department of Earth Sciences, National Central University, Zhongli, Taiwan

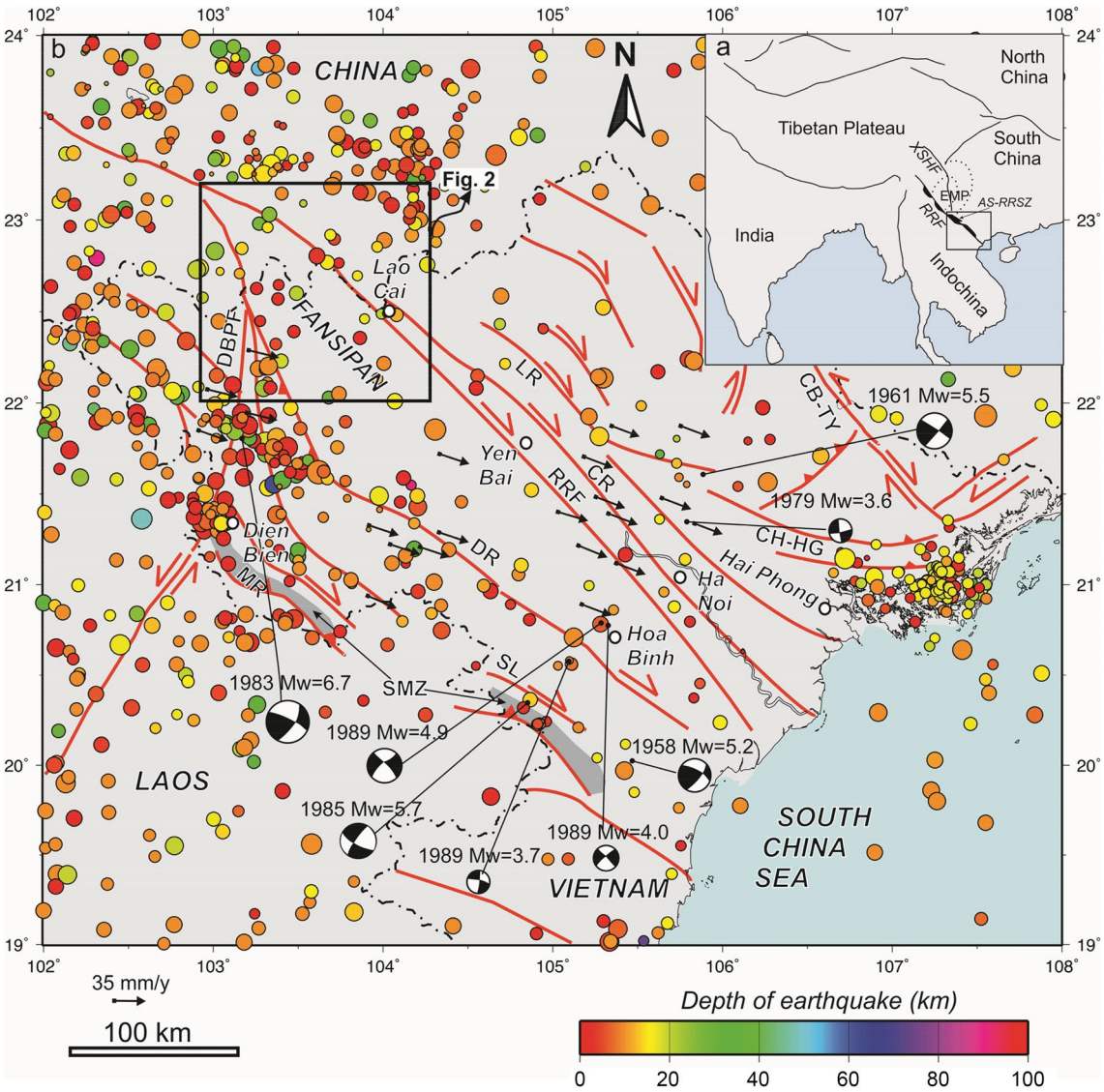

Fig. 1 **a** Tectonic map showing locations of major plates related to the collision of India and Eurasia. Black lines indicate major faults. Dash lines indicate different zones related to the Emeishan Mantle Plume. Black area represents the location of the Ailao Shan-Red River shear zone. The abbreviations of names are as follows: *RRF* Red River Fault, *AS-RRSZ* Ailao Shan-Red River shear zone, *XSHF* Xianshuihe Fault, *EMP* Emeishan Mantle Plume. **b** Active fault systems and seismicity of northern Vietnam, after Tran et al. (2013). Seismic events (1980–2016) were downloaded from the website https://www.isc.ac.uk. The colors of the circular symbols indicate different depths of earthquakes. The size of the symbol indicates the earthquake magnitude (Mw 1.0–5.1). Focal mechanisms of the earthquake data (1903–1990) were from the published study of Cong and Feigl (1999). The red lines indicate faults. The red arrows show the directions of movement along the strike-slip faults. The black arrow indicates GPS vectors after Tran et al. (2013). The dark-grey area indicates the location of the Song Ma zone (SMZ). The abbreviations of fault names are as follows: *DBPF* Dien Bien Phu fault, *MR* Ma River fault, *DR* Da River fault, *SL* Son La fault, *RRF* Red River fault, *LR* Lo River fault, *CR* Chay River fault, *CH-HG* Chi Linh-Hong Gai fault, *CB-TY* Cao Bang-Tien Yen fault. The location of the study area is shown in the rectangle

research papers have explored the tectonic activities of the RRF and the DBPF (Allen et al. 1984; Wang et al. 1998; Schoenbohm et al. 2004; Lai et al. 2012; Duong et al. 2013; Zuchiewicz et al. 2013), studies regarding the tectonic deformation of the wide Fansipan mountain range remain limited. A detailed investigation of tectonic deformation in the Fansipan mountian range is necessary to improve our knowledge about recent tectonic movements in the greater area of northern Vietnam.

While the deformation structures of northern Vietnam are mainly controlled by strike-slip faulting (Fig. 1) with a dominant horizontal movement, the Fansipan mountain range comprises high mountains among well-known strike-slip lineaments. Therefore, the question raised is what is the

main tectonic mechanism responsible for the high topography of the Fansipan mountain range, and whether the deformation of the Fansipan mountain range and the movement of strike-slip faulting are related. In this study, methods of tectonic geomorphology are applied to extract information regarding the patterns of active deformation in the Fansipan region. First, DEM data derived from satellite imagery are utilized to generate interactive 3D perspective views of the topographic surface. Features that are representative of recent active fault activities, such as offset of mountain ridges or rivers, consistent sharp triangular facets, straight linear features that crosscut lithological boundaries are used to map possible fault traces in the Fansipan mountain range. Furthermore, field investigations were carried out in accessible places to verify the mapped fault scarps or traces. We investigated lineaments through exposed outcrops where offset of rocks or fault slickensides can be observed. Second, river systems in the Fansipan mountain range are analyzed through river profiles as well as their normalized steepness index values to infer the relative uplift pattern. Third, kinematics and associated stress field of the mapped fault systems in the field are documented and analyzed. Combining the aforementioned approaches, we attempted to explore the mechanism that may be responsible for the sustained high topography of the Fansipan mountain range, as well as to understand recent tectonic movements that are still unclear in northern Vietnam.

Geological background

Northern Vietnam is a part of the Indochina and South China plates resulting from the Permian–Triassic Indosinian Orogeny. The boundary between the South China and Indochina plates is classically represented by the Ailao Shan-Red River shear zone (AS-RRSZ) (Tapponnier et al. 1986). However, since ophiolites and eclogites were discovered, the Song Ma zone has been interpreted as a suture zone between the South China and Indochina plates (Shu et al. 2008; Zhang et al. 2013; Faure et al. 2014). As a result, a large part of northern Vietnam was affected by the Indosinian Orogeny event during the Permian–Triassic Time. During the Cenozoic, tectonic structures of northern Vietnam were dominated by the development of many strike-slip faults. Among the strike-slip faults, the RRF and DBPF have been intensively studied during recent decades (Allen et al. 1984; Wang et al. 1998; Schoenbohm et al. 2004; Cong Duong et al. 2006; Lai et al. 2012; Zuchiewicz et al. 2013). The RRF, commonly associated with the indentation of the India plate into the Eurasia plate, is one of the most significant discontinuities in SE Asia. In this study, we restrict the use of the name RRF as an active strike-slip fault and consider the RRF to be a separate structure from the left-lateral shearing of the older AS-RRSZ. The geomorphic and geologic data (Allen et al. 1984; Wang et al. 1998; Schoenbohm et al. 2004) indicate that the RRF is currently undergoing transtensional deformation with a combination of normal and right-lateral strike-slip movements. The DBPF is the most seismically active fault in northern Vietnam (Fig. 1). The north- to northeast-trending DBPF connects to the Xianshuihe Fault, which is a large strike-slip fault in southwestern China. It has been proposed that the movement of the DBPF is related to the Xianshuihe Fault with the same slip sense and spatial alignment (King et al. 1997; Chen et al. 2000; Shen et al. 2005). Current geomorphologic and geodetic data indicated that the DBPF is an active left-lateral strike-slip fault (Cong Duong et al. 2006; Lai et al. 2012).

Among these active faults, the Fansipan mountain range is a high topographic region, stretching in the NW–SE direction, parallel to the strike of the RRF (Fig. 2). Formed in a complicated tectonic region, the Fansipan mountain range has a long geological history. The Fansipan's rock ages range from the Precambrian to the Cenozoic (Lan et al. 2001; Nam 2001; Dung et al. 2012; Usuki et al. 2015; Tran et al. 2015). Most of the rock types in the Fansipan mountain range are granitoids; the remainder are volcanic, sedimentary, and metamorphic rocks that occupy small parts in the central region and outer edges of the mountain. Petrogenesis analysis (Usuki et al. 2015; Tran et al. 2015) has indicated that the Late Permian plutonic rocks of the Fansipan mountain range have a genetic relationship with the alkaline granites of the inner zone of the Emeishan Mantle Plume (EMP) in China. The formation of the Fansipan magmatic rocks has been interpreted to be related to the EMP, and the movement of the Fansipan block to the current position is the consequence of the left-lateral shearing along the AS-RRSZ (Tran et al. 2015). Even though lots of research has been done to investigate petrology, geochemistry and geochronology of the Fansipan mountain range (Tapponnier et al. 1990; Leloup and Kienast 1993; Leloup et al. 2007; Usuki et al. 2015; Tran et al. 2015), the recent tectonic movements of this high mountainous area are less well understood. In this study, we used new Advanced Spaceborne Thermal Emission and Reflection Radiometer (ASTER) 30-m digital elevation models (DEMs) for the tectonic analysis of the Fansipan mountain range.

Methodology

This study analyzed 30-m resolution DEM data derived from ASTER imagery (https://gdem.ersdac.jspacesystems.or.jp/search.jsp) to interpret the geomorphic characteristics of the Fansipan mountain range. With the ArcSence 10.2 software, an interactive 3D perspective view allows one to easily visualize the pattern of surface deformation and interpret the

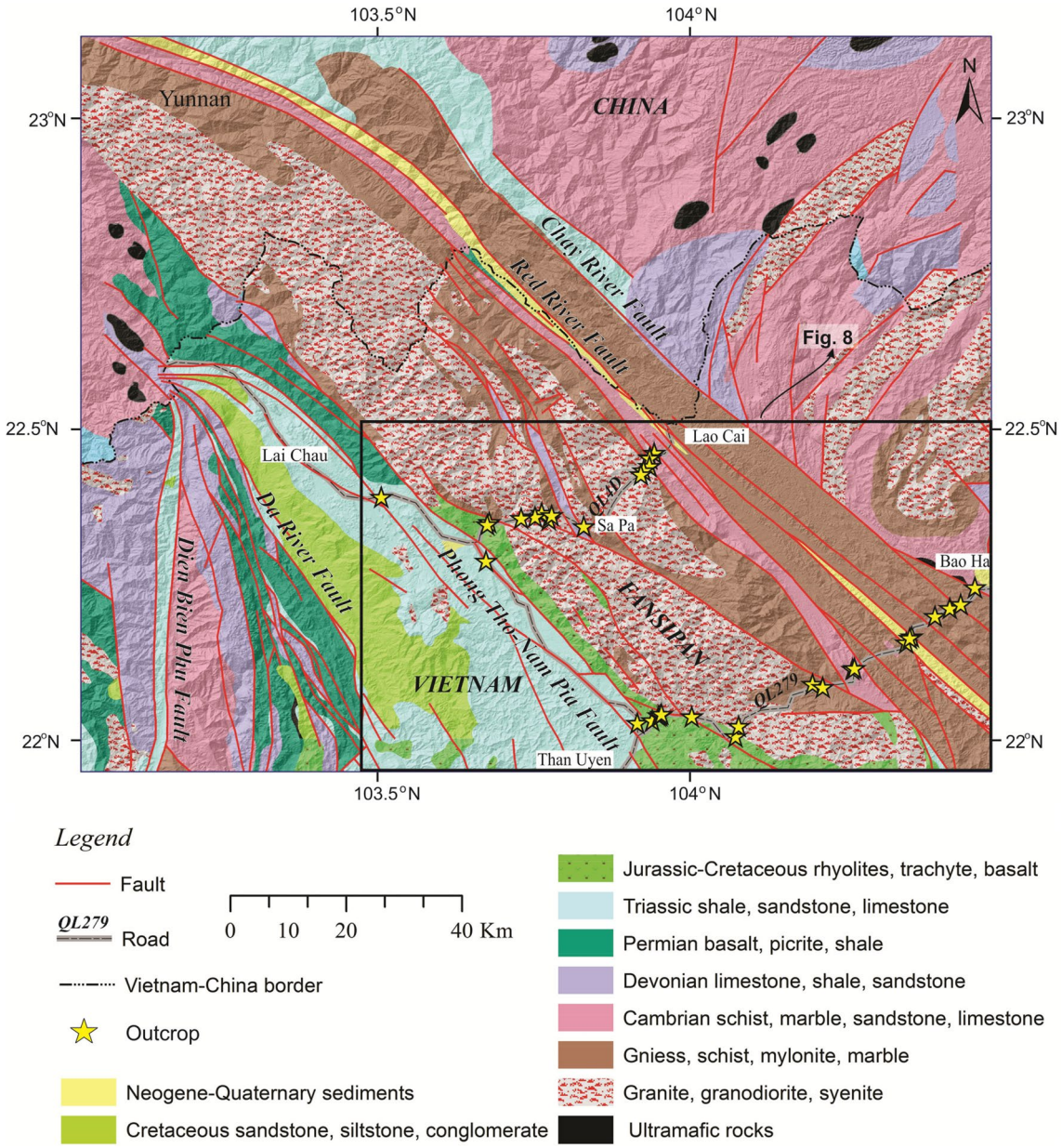

Fig. 2 Simplified geological map of the Fansipan mountain range and adjacent regions. The geologic units were regrouped to better illustrate the regional geology. The map was compiled and simplified from the geological maps of China (Zhou et al. 2013) and Vietnam (1:1,500,000 geological map from General Geological Department of Vietnam, 1983). The name of outcrop was described in Fig. 8 as shown by black rectangle

existence of major faults, which played an important role in understanding the recent movements of the study area. To detect the change of elevation of the topographic surface, the swath profiles have been analyzed within the Fansipan mountain range. The swath profiles were automatically delineated showing statistical values such as the minimum, mean, and maximum of elevation using the Swath Profiler tool in the ArcGIS software.

To obtain a tectonic signal on the different sides of the mountain range, we focused on analyzing the river profiles of channels that have a longitudinal trend perpendicular to the trend of the mountain range. Although river channels occupy a small part of the land surface, a longitudinal river profile is a more sensitive indicator of rock uplift rate than other morphological properties (Whipple 2004). A common procedure for river network extraction is described briefly in the following. The ASTER DEM data can be downloaded for free from the website https://gdem.ersdac.jspacesystems.or.jp/search.jsp. Once the DEM data have been obtained, pits and holes in the DEM need to be filled to create raster

files of flow direction and then flow accumulation. Using a threshold value, a river network can be delineated using the data from the raster file of flow accumulation. All these steps can be processed using the Hydrology tools in the ArcGIS software. In this study, the threshold drainage value of 10^5 m^2 was used for automated river network delineation. The quality of the delineated river network is highly dependent on the quality of the used DEM data. In this study, the ASTER 30-m DEM was used for automated extraction of the river network in the Fansipan mountain range. Based on some studies (e.g. Mukherjee et al. 2012; Santillan and Makinano-Santillan 2016), the vertical accuracy of elevation from the ASTER 30-m DEM in the Root Mean Square Error (RMSE) ranges from 11.98 to 12.62 m. Although the studies about the accuracy of elevation are not comprehensive, they give an estimate about the quality of the used DEM data. The vertical accuracy of elevation is applicable to our study in terms of the vertical scale and it may reflect the quality of the river network values presented in this study. Once the river network has been created, a suite of Matlab codes downloaded from the website https://geomorphtools.geology.isu.edu/Tools/StPro/StPro.htm can be used to extract river profiles.

To extract quantitative information on the rock uplift rate, we also calculated the normalized steepness index of the rivers. The value of the normalized steepness index can be affected by lithology. The contrasting lithology between the Fansipan mountain range and its surrounding areas may lead to differences in the normalized steepness index. However, in this study, the normalized steepness index was mainly analyzed within the Fansipan mountain range where the dominant lithology is plutonic rocks from the EMP. Thus, the similar lithology within the Fansipan mountain range is considered to have minimal influence on the differences of the normalized steepness values in this study. The analysis of normalized steepness index followed the method of Wobus et al. (2006) and Whipple et al. (2007). The fundamental idea is that the relative change in elevation is balanced with uplift and erosion. The change in elevation can be expressed as the following equation:

$$\mathrm{d}z/\mathrm{d}t = U(x,t) - \varepsilon(x,t), \tag{1}$$

where $\mathrm{d}z/\mathrm{d}t$ defines the change in elevation according to time, x is the horizontal distance along the river, U is the rock uplift rate, and ε is the erosional rate. However, the erosional rate ε is often expressed as a power law function of the drainage area (A) and slope gradient (S) as follows:

$$\varepsilon = KA^{m}S^{n}, \tag{2}$$

where K is a dimensional coefficient of erosion, and m and n are positive constants related to the basin hydrology, hydraulic geometry, and erosional process (Howard et al. 1994; Whipple and Tucker 1999). Under a steady-state condition ($\mathrm{d}z/\mathrm{d}t = 0$), with a uniform U and K and constant m and n, Eqs. (1) and (2) can be solved for the equilibrium slope (S_e) as follows:

$$S_e = (U/K)^{1/n}A^{-m/n} = k_sA^{-\theta}, \tag{3}$$

where θ describes the concavity of the river and the coefficient $(U/K)^{1/n}$ is the river steepness index. The steepness index (k_s) and concavity (θ) are determined by a linear regression of the slope (S) and area (A) data. To compare rivers of different areas, the steepness index can be normalized into the normalized steepness index (k_{sn}) using a fixed reference concavity (θ_{ref}). In our study, we used a reference concavity (θ_{ref}) of 0.45 for all channels analyzed. This value is a typical value of concavity of equilibrium bedrock channels under conditions of uniform uplift (Snyder et al. 2000; Kirby and Whipple 2001). Combining the Matlab and ArcGIS programs, the normalized steepness index can be shown on a spatial map to readily compare the values of different areas. All codes for running the program were downloaded from https://geomorphtools.geology.isu.edu/Tools/StPro/StPro.htm.

In addition to using digital topographic data to extract quantitative information regarding the tectonics, we also conducted field investigations to observe and measure active deformation of the Fansipan mountain range and surrounding areas. Some field photographs containing indicators of fault striations to delineate fault movement are shown in Fig. 3. In the field, we focused on recognizing fault planes and identifying the sense of relative movement as well as slickenside striations to obtain the stress field of the study area. The measurement data were analyzed by a computer program using the inverse method as described in detail by Angelier (1979, 1989, 1990) and Angelier et al. (1982). The assumption of the inverse method is that all faults moved independently but consistently under a single homogeneous stress regime expressed by a unique stress tensor. The stress tensor is calculated using a set of field data, including the strike and dip of several faults and the directions and senses of slip on these fault surfaces (as indicated by slickenside striations). The orientations of the three principal stress axes (maximum—σ_1, intermediate—σ_2, maximum—σ_3) and the ratio Φ of the differences of the three principle stresses ($\Phi = (\sigma_2 - \sigma_3)/(\sigma_1 - \sigma_3)$) are thus determined. In this study, we mainly focus on measuring the fault slip data at two transects across the Fansipan mountain range, along road QL4D from Lao Cai city to Sa Pa town and along road QL279 from the Than Uyen district to Bao Ha district.

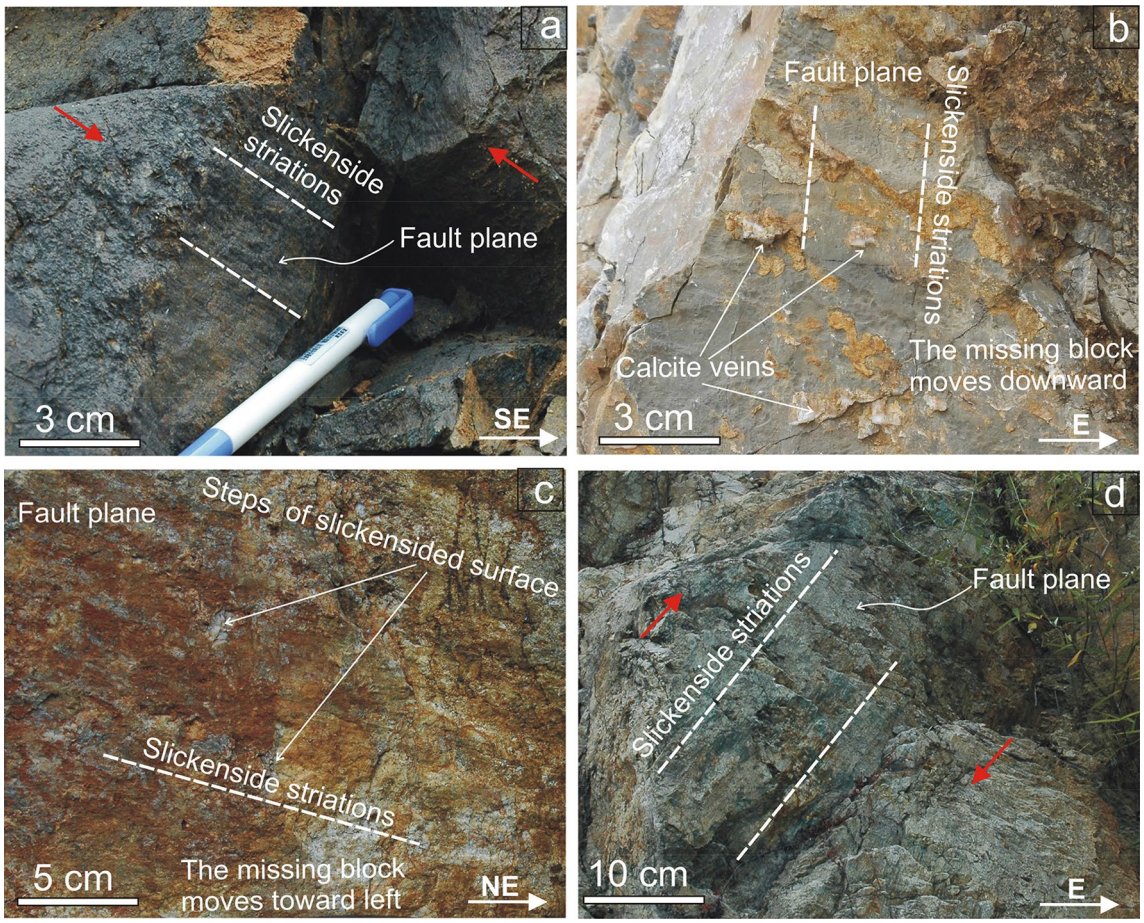

Fig. 3 Field photographs showing fault traces and slickenside striations of some outcrops. The red arrow indicates the direction of rock movement on the opposite sides of the fault plane. The white dashed line indicates the orientation of the striations on the slickenside. **a** Field photograph taken from outcrop 02–01 indicating right-lateral strike-slip movement. **b** Calcite veins on the fault plane suggesting normal fault movement in outcrop 08–23. **c** Fracture steps on the fault plane indicating right-lateral strike-slip movement in outcrop 02–04. **d** Slickenside striations and fracture geometries on the fault plane suggesting right-lateral strike-slip movement on outcrop 02–05. The outcrop locations are shown in Fig. 8

Results

Topographic analysis

Topographic and field observations

In this study, topographic lineaments and surface features have been visualized and recognized based on interactive 3D perspective views derived from the ASTER 30-m DEM. To overcome the existence of anomalies and artifacts from the DEM, we utilized Google Earth images for more detail in searching topographic features. These topographic features had also been compared with previous mapped faults from the geological map and published studies. Most importantly, field investigations had been carried out to verify whether the mapped topographic features are proper faults or not. Combining the ASTER 30-m DEM, Google Earth images, geological maps and field observations, we identified and remapped new linear locations of faults within and surrounding the Fansipan mountain range (Fig. 4). The NE and SW sides of the Fansipan mountain range are bounded by two major faults: the RRF and the Phong Tho-Nam Pia Fault. Both strike NW–SE and are parallel to the trend of the mountain range. The north- to northeast-trending DBPF appears to the west of the mountain range. Within the mountain range, minor faults cut and divide the Fansipan mountain range into smaller portions.

From the ASTER 30-m DEM imagery, we noticed that the topographic features of the Fansipan mountain range are heterogeneous from the north to the south (Fig. 4a). In the north part, the shape of the topography tends to be symmetrical with the crests of the mountain in the middle of the range. However, in the south part, the topographic shape becomes asymmetrical with the crests nearer the SW side of the mountain range. The topographic variation in the Fansipan mountain range was further confirmed by the swath

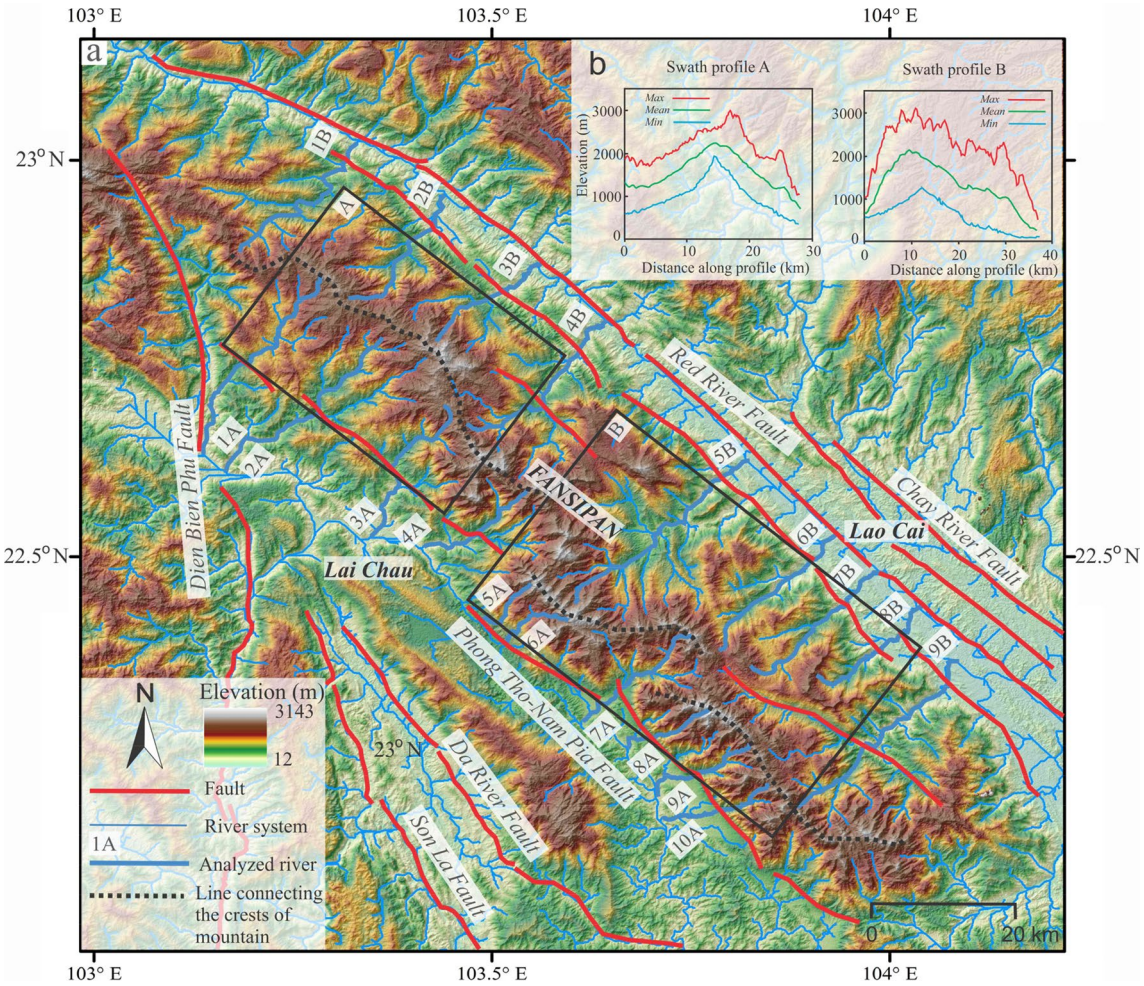

Fig. 4 **a** Topographic map showing river system and distribution of major and minor faults (red lines) within the Fansipan mountain range and surrounding regions. The blue line indicates river. The number before the river labels the name of the river used for river profile and normalized steepness index analyses. Dash line indicates line connecting the crests of mountain. **b** Swath profiles (for their locations see **a**) showing the maximum, mean, and minimum elevation. The swath profile of the north part of the Fansipan mountain (profile A) shows a symmetrical form of land surface with a similar topographic relief on both sides of the mountain range. In the south part, the crests of the mountain shift to the SW side. The swath profile of the south part of the Fansipan mountain range (profile B) shows an asymmetrical form with a steep slope on the SW side and a gentle slope on the NE side

profile analysis (Fig. 4b). The swath profile extracted from the north part shows a symmetrical form with a high elevation in the middle part and similar slope on both flanks of the profile. However, in the south part, the swath profile shows an asymmetrical form with steep and high relief on the SW flank and gentle and low relief on the NE flank. Altogether, our geomorphic analysis revealed a significant asymmetrical form of the Fansipan mountain range, which may be indicative of movements of the fault systems underlying it.

Moreover, on the SW side in the south part of the Fansipan mountain range along the inferred Phong Tho-Nam Pia Fault, there are well-developed triangular facets that are easily observed in the field as well as from 3D perspective views derived from ASTER DEM (30 m) (Fig. 5). Triangular facets are topographic features frequently observed at normal fault scarps. The development of triangular facets and the fresh surface without vegetation cover on the fault scarp is shown in Fig. 5c. It suggests recent movements of the inferred normal faulting along the Phong Tho-Nam Pia Fault. In addition, a pronounced topographic contrast such as a steep and high escarpment of a mountain and a gentle slope of alluvial fans occurring across the inferred Phong Tho-Nam Pia Fault suggests a range-front fault scarp on the SW side in the south part of the Fansipan mountain range. The gentle topography on the SW side of the inferred Phong Tho-Nam Pia Fault may be a result of subsidence of the hanging wall and deposition of alluvial sediment covering the top of the footwall. From our observations, we considered the Phong Tho-Nam

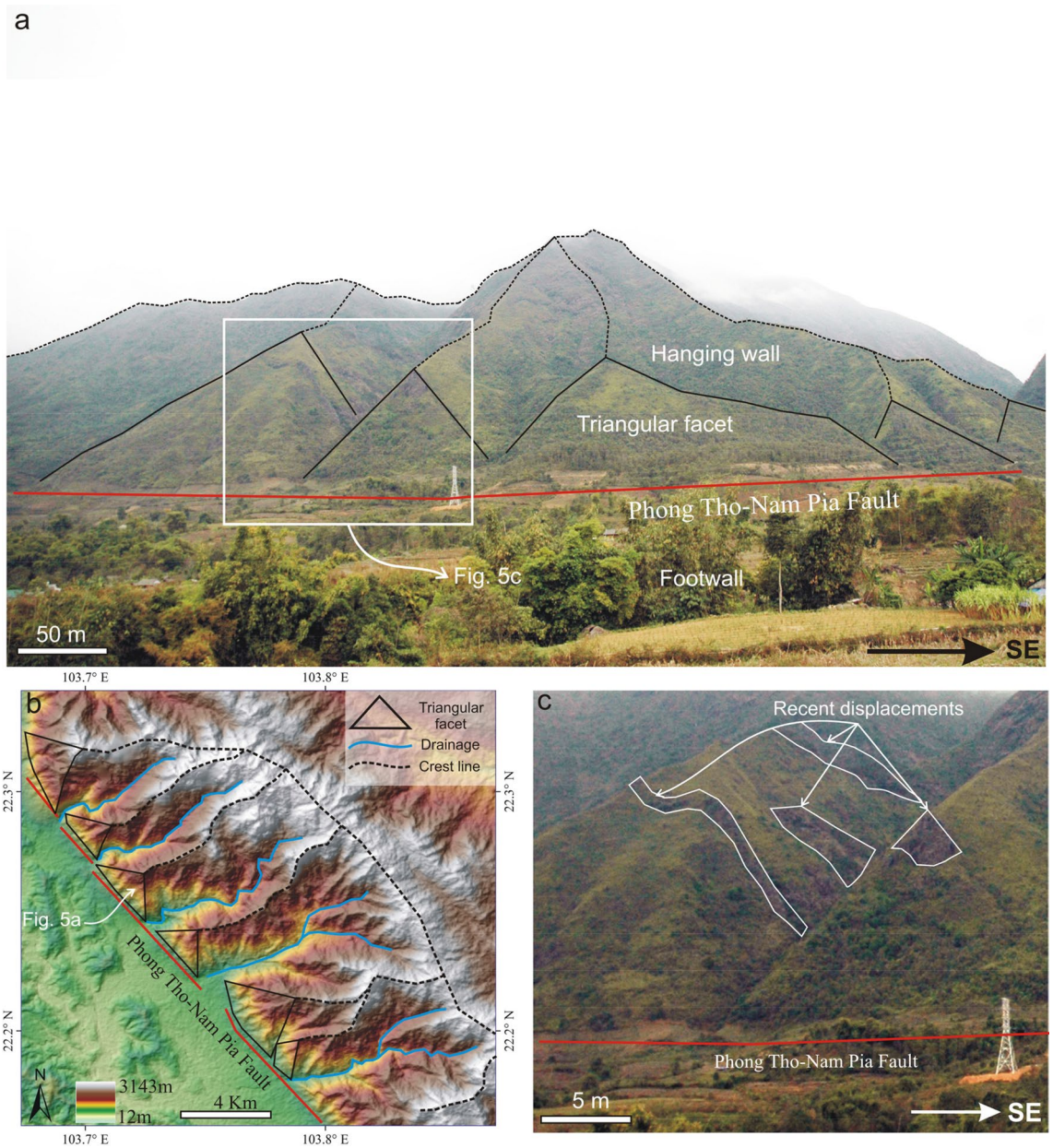

Fig. 5 Field photographs (**a**, **c**) and topographic map (**b**) showing geomorphic indicators of active normal faulting along the Phong Tho-Nam Pia fault. **a** Landform indicators of normal movement along the Phong Tho-Nam Pia fault including the fault trace, triangular facets, flat alluvial surface in the footwall, and high relief of the mountain in the hanging wall. **b** Topographic map of the SW flank on the south part of the Fansipan mountain range, generated from ASTER 30-m DEMs, showing a pattern of triangular facets along the Phong Tho-Nam Pia fault. The red line represents the active fault trace. **c** Zooming in photograph of (**a**) shows well exposed fault scarps with fresh surface with minimal plant cover indicating recent normal faulting

Pia Fault to be a tectonically active fault that bounded the footwall mountain range. Although no large earthquakes resulting from slip along the inferred Phong Tho-Nam Pia Fault have been recorded since 1980, the youthful landforms with newly formed fault scarps suggest that it may generate large earthquakes in this area in the future.

Analysis of longitudinal river profiles

The longitudinal profiles of 19 rivers have been extracted using 30-m DEM data (Fig. 6). The prominent topographic appearance of the Fansipan mountain range is expressed by a symmetrical form of topography in the north part and an asymmetrical form in the south part as shown in Fig. 4b.

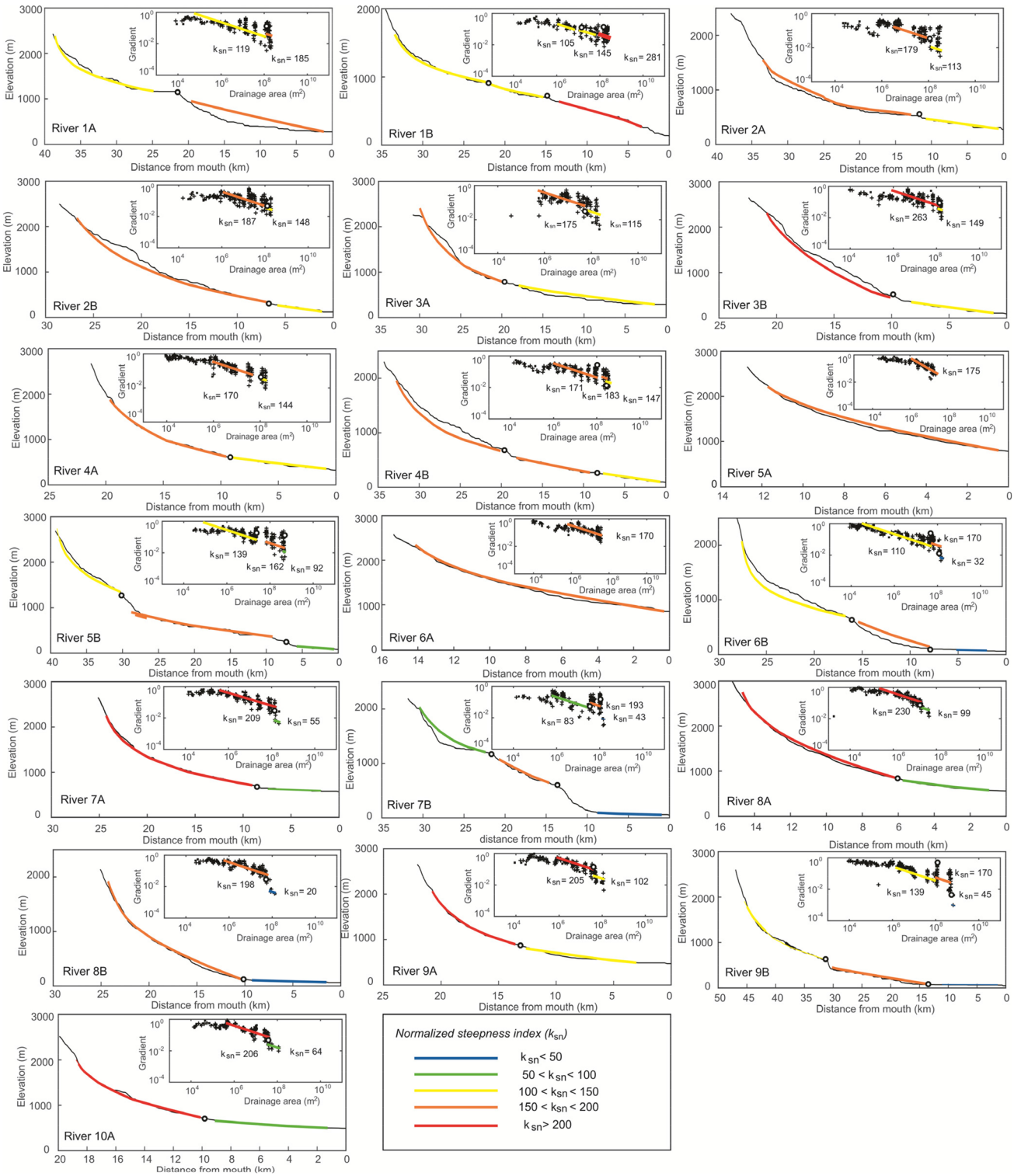

Fig. 6 Longitudinal profiles and log–log plots of gradient versus drainage area of the analyzed rivers. The locations of the analyzed rivers are shown in Fig. 4a. The knickpoints separating river segments are shown as black circles (both on the longitudinal profiles and log–log plots). The colored lines represent the regressed segments of rivers. Different colors represent different values of normalized steepness index (k_{sn})

Based on this characteristic, we classified the rivers of the Fansipan mountain range into two regions: the north part includes rivers 1A, 2A, 3A, and 4A on the SW side and rivers 1B, 2B, 3B, and 4B on the NE side, and the south part includes the remaining rivers. The names of the rivers and their positions are shown in the topographic map of Fig. 4a. The analysis of longitudinal river profiles based on some morphologic features such as shape, length, and slope gradient. We recognized that in the north part, the morphologic features of the rivers on both sides of the mountain are quite similar. The length of the rivers on both sides ranges from 20 to 40 km. The slope gradient and the shape of the rivers on both sides are also similar. In contrast, in the south part, the river profiles are very different from the SW to the NE sides of the mountain range. While the rivers on the SW side are steep and short, the rivers on the NE side are long and gentle. In particular, all the rivers on the SW side in the south part are less than 25 km in length; however, the length of the rivers on the NE side in the south part range from 20 to greater than 40 km. Furthermore, reviewing the elevation of the downstream area, all of the rivers on the SW side in the south part have a minimum elevation higher than 400 m, while the minimum elevation of the other rivers on the NE side is lower than 300 m. The different elevations may be a consequence related to different uplift patterns on different sides of the mountain.

Analysis of normalized steepness index (k_{sn})

To obtain tectonic information about the uplift pattern of the Fansipan mountain range, the normalized steepness index (k_{sn}) values have been calculated along 19 selected rivers. The k_{sn} values along the individual rivers are shown in Figs. 6 and 7. Each river shows one to three different k_{sn} values related to different regressed segments separated by the river's knickpoints. In general, high values of k_{sn} of more than 200 $m^{0.9}$, indicated by the red color in Figs. 6 and 7, are much more common on the SW side of the south

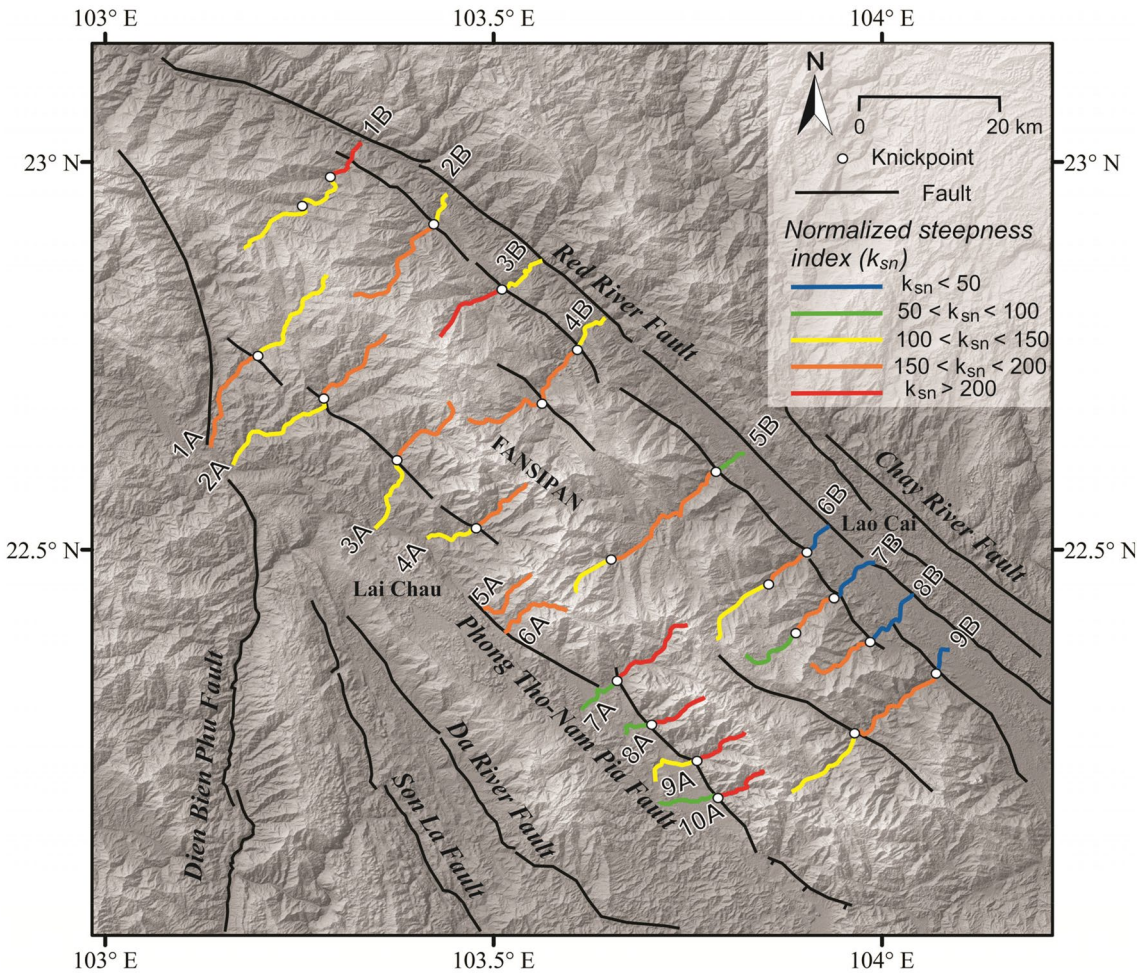

Fig. 7 Topographic map showing the normalized steepness index (k_{sn}) values and the locations of knickpoints along the rivers as indicated in Fig. 6. The different colors represent different values of k_{sn}

part of the mountain range adjacent to the Phong Tho-Nam Pia Fault. In contrast, on the other sides of the mountain range, only a few river segments have high values of k_{sn}. Most of the river segments on these sides show relatively low k_{sn} values ranging from 20 to less than 200 $m^{0.9}$. In addition to the steepness index, we also determine knickpoints in terms of both channel profile and slope-area scaling (Wobus et al. 2006 and Kirby and Whipple 2012). If knickpoints are selected using only channel profiles, we may obtain several knickpoints that are tectonically irrelevant. However, if we consider the log–log diagrams of slope and area as shown in Fig. 6, the knickpoints can be significantly reduced and provide relevant information about tectonic uplift as argued in Wobus et al. (2006). Based on the longitudinal profiles and the log–log diagrams of the slope and area data, we identified 23 major knickpoints along the main rivers flowing cross the Fansipan mountain range. Most of the identified knickpoints locate at variable elevations and they are spatially associated with the location of faults, which clearly separate the zones of the high and low k_{sn} values.

Analysis of stress field

To investigate the orientation of the stress field in the Fansipan mountain range and understand the patterns of tectonic deformation, we measured fault slip data at two transects within the study area. The results of the stress investigation using fault kinematics are shown in Fig. 8. The Fansipan mountain range and its vicinity are characterized by three main sets of stress pattern. The first pattern is a set of nearly horizontal maximum principal stress (σ_1) trending NW–SE and minimum principal stress (σ_3) trending NE–SW, which is pervasive across the entire regions. Notably, this kinematic pattern is consistent with the published GPS data (Tran et al. 2013; Minh et al. 2014) for recent strike-slip movements in northern Vietnam. The second pattern is a set of a vertical to sub-vertical maximum principal stress (σ_1) and horizontal minimum principal stress (σ_3), which is observed in some outcrops such as 08–07; 08–21; 08–22; 08–24; 08–26; 08–28; 08–32 as shown in Fig. 8. This orientation of stress pattern is in good agreement with the topographic observations in explaining the normal faulting activity along the Phong Tho-Nam Pia Fault. The third pattern is a complex system of mixture between the strike-slip and normal motions. The orientations of the maximum principal stress (σ_1) and the intermediate principal stresses (σ_2) are not tightly constrained while the orientation of the minimum principal stress (σ_3) is consistently in the direction of NE–SW and nearly horizontal as observed in the outcrops: 02–02; 02–03; 02–05; 08–06; 08–29; 08–30.

Discussion

Deformation pattern of the Fansipan mountain range

The Fansipan mountain range is near the boundary between the Indochina and South China plates that has a complex tectonic setting and geological history. Although there has been some research completed regarding the petrology and geochronology of the Fansipan mountain range (Leloup et al. 2001; Usuki et al. 2015; Tran et al. 2015), investigation and analysis of the tectonic deformation has been limited. The topolineaments within the Fansipan mountain range and its surrounding areas have been preliminarily interpreted using LANDSAT images and SRTM data (Zuchiewicz et al. 2013); however, the low resolution of DEM data may hinder the mapping precision of geomorphic features. Instead of using SRTM 90-m DEM data, the ASTER 30-m DEM data were used in this study to identify the geomorphic features in the Fansipan mountain range with a desirable precision. In addition, field investigations were carried out to re-examine the geomorphic features inferred from the higher resolution DEM data. Combining the ASTER 30-m DEM data and field observations, we identified and remapped new locations of faults more precisely as compared to those of the previous study.

Utilizing the ASTER 30-m DEM imagery, we recognized that the topographic surface of the Fansipan mountain range is spatially variable with steep and high relief on the SW side of the south part. The interaction between the tectonics and the topographic surface has been discussed in many previous studies (Whipple et al. 2007; Burbank et al. 2011; DiBiase et al. 2012; Escamilla-Casas and Schulz 2016). It is possible to infer differential tectonic deformation from variations in the topographic surface. In the past, some case studies using the change in surface topography to constrain fault movements beneath the surface have been completed (Burbank et al. 2011; Kirby and Ouimet 2011). For example, an asymmetrical form of surface topography in the Himalaya can be interpreted as a result of a thrust-generated mountain range as mentioned in the CHILD model (Burbank et al. 2011). Therefore, the topographic variation in the Fansipan mountain range in our study may be related to distributed faults underlying the mountain range.

Rivers are a sensitive geomorphic indicator from which meaningful tectonic information can be extracted. The divide of drainage basins is strongly shifted from a middle position toward an active normal fault (Leeder and Jackson 1993). Thus, among the most important criteria to distinguish the relative activity of different flanks of

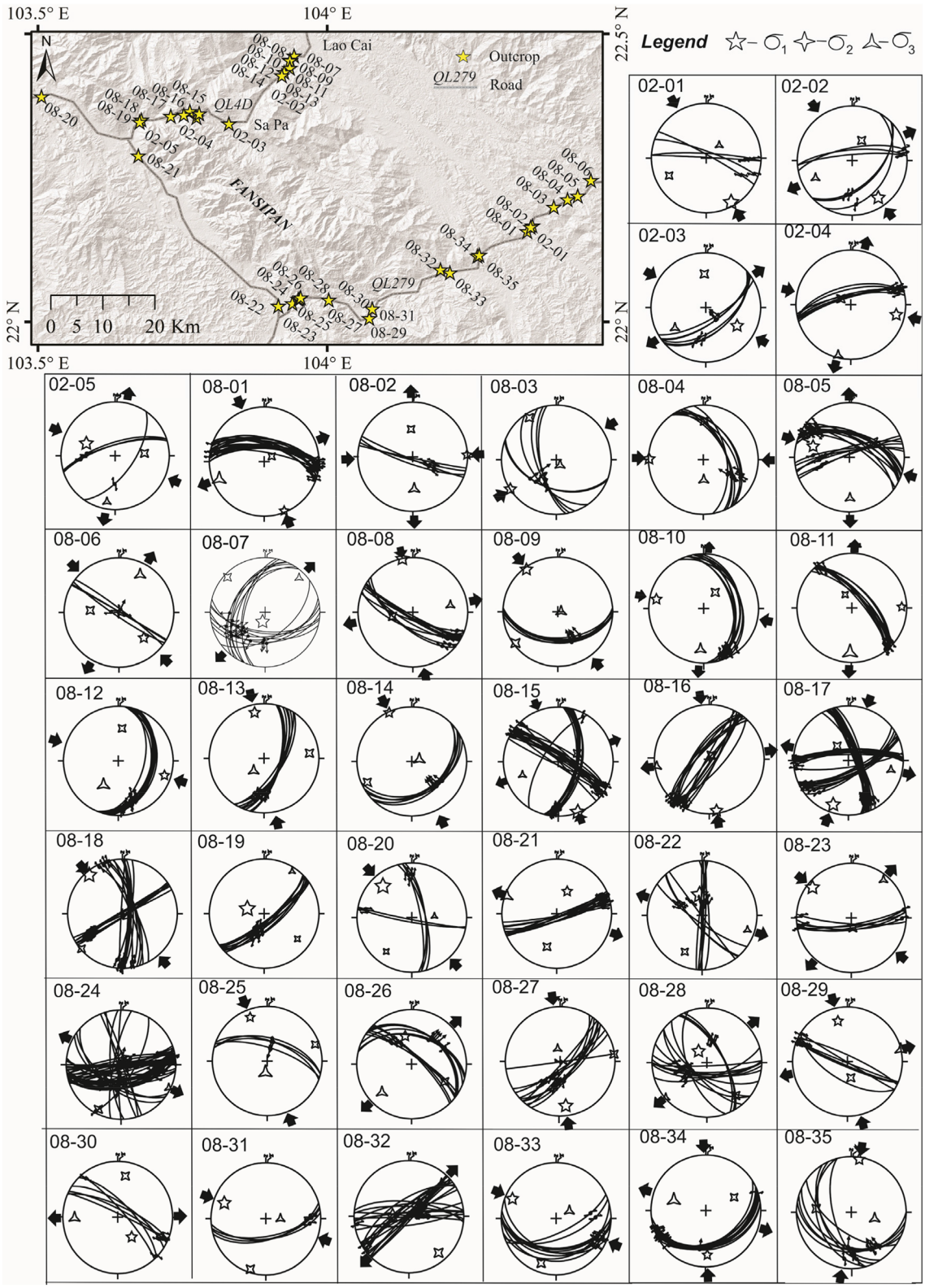

Fig. 8 Topographic map showing outcrop locations and stress reconstructions around the Fansipan mountain range and surrounding areas. Fault planes are represented by solid lines and slickenside striations are represented by small dots with arrows indicating the sense of motion (double arrows for strike-slip, outward-directed arrows for normal slip, and inward-directed arrows for reverse slip). The inversion of fault slip data followed the method of (Angelier 1990). The axes of maximum principal stress (σ_1), intermediate principal stress (σ_2), and minimum principal stress (σ_3) are 5-, 4- and 3-branch stars, respectively. The large black arrows indicate the trend of compression and/or extension

mountain ranges bounded by different fault systems is to examine the size and the slope of the rivers on both sides. The result from our analysis indicates that the rivers on the SW side of the south part of the Fansipan mountain range are shorter and steeper compared to those on other sides. The length of the rivers on the other sides ranges from 20 to 40 km, while nearly all the rivers on the SW side in the south part are less than 25 km in length. The relatively short and steep rivers on the SW side in the south part of the Fansipan mountain range resemble those of normal faulting regions described in the case study of Leeder and Jackson (1993). The resemblance between the data from the published research and our study suggests a normal faulting activity on the SW side in the south part of the Fansipan mountain range.

The value of the steepness index of river systems can be affected by both tectonic and non-tectonic factors. The non-tectonic factors, such as lithology, climate and base-level change, are possibly important factors in changing the shape of topography. Contrasting lithology may lead to differences in rock erodibility that may affect the steepness value of rivers or produce knickpoints. Nonetheless, the petrologic studies (Usuki et al. 2015; Tran et al. 2015) indicate that the dominant lithology of the Fansipan mountain range is plutonic rocks with the same petrologic origin from the EMP in China. Therefore, the influence of lithology is considered minimal on the spatial variation of steepness values within the Fansipan mountain range. Climate change, especially the variation in precipitation, is a possible mechanism for knickpoints to form and can affect the values of the steepness index. The average annual precipitation (Vu et al. 2018) shows almost similar values within the Fansipan mountain range and the data of climate change during the last 50 years (Schmidt-Thomé et al. 2015) were also similar within the region. Thus, to the best of our current knowledge, the climate change is interpreted to have minimal influence on the spatial variation of steepness index within the Fansipan mountain range. The base-level change is also among the factors for knickpoint formation or affecting the steepness index values along the rivers. If the perturbation by the base-level change occurs, we expect to observe transient river systems with a set of knickpoints in the river profiles at almost similar elevations (Niemann et al. 2001; Wobus et al. 2006). However, we did not find such patterns of knickpoint locations in the Fansipan mountain range. Thus, we consider that the tectonic process is the dominant factor driven the topography as well as the spatial variation in the steepness index of the Fansipan mountain range. The results from our analysis show a considerable variation in the normalized steepness index among the different areas of the Fansipan mountain range. The region of high normalized steepness index is mostly distributed on the SW side of the south part of the Fansipan mountain range. The variation in the distribution of the normalized steepness index can provide constraints on the inferred uplift pattern of the range. The high steepness index on the SW side in the south part of the range suggests a high rock uplift rate on this side compared to that of the other sides.

Overall, the results from our analysis show a significant correlation between topography, river profile, and normalized steepness index that allow us to preliminarily interpret the deformation pattern of the Fansipan mountain range. We, therefore, infer that the uplift pattern of the range is spatially variable with a higher uplift rate on the SW side of the south part near the Phong Tho-Nam Pia Fault.

Co-existence of normal and strike-slip faulting and interpretation of stress permutation

Two main fault systems were observed to be distributed within and surrounding the Fansipan mountain range. The first fault system is dominated by strike-slip faults that were found in veins and brittle slickenside surfaces in the field. The stress pattern is compatible with a nearly horizontal maximum principal stress (σ_1) trending NW–SE and minimum principal stress (σ_3) trending NE–SW. The stress pattern is also consistent with recent right-lateral and left-lateral strike-slip movements of the RRF and the DBPF, respectively. The second fault system is dominated by normal faults as suggested by the stress pattern of the vertical to sub-vertical maximum principal stress (σ_1) and horizontal minimum principal stress (σ_3) at approximately NE–SW direction. The normal fault system is also suggested by the topographic observation and river profile analysis. The two main fault systems in the Fansipan mountain range are likely active in recent geologic time based on the following reasons. First, topographic observations and river profile analyses show aspects of tectonic geomorphology that record surface deformations at the time scales ranging from days to millions of years (Burbank et al. 2011). The observed topography-related data in the Fansipan mountain range are most relevant to the youngest deformations that have changed the geomorphic surface of the study area. Second, our field investigation indicates youthful landforms with clear and sharp offsets of mountain ridges. There is little vegetation cover within the observed fault scarps suggesting that these faults were displaced recently and being tectonically active. Third, the stress investigation from our field survey indicates that almost all the observed faults have shown brittle deformation. The brittle-natured faults should have recorded deformation at relatively shallow depths and subsequently being uplifted onto the surface. The brittle deformation and youthful fault scarps observed from the field suggest that the analyzed faults have been displaced recently. Although both the normal and strike-slip faults are considered to be active, the timing relationship between these faults is not

obvious. Based on the cross-cutting relationship, some outcrops indicate earlier movement of normal faulting than that of strike-slip faulting, whereas others indicate the opposite. To properly interpret the combination of the observations in topography and stress patterns, we proposed that the Fansipan mountain range may experience a permutation of σ_1/σ_2 under the same extensional stress regime of minimum principal stress (σ_3) that trends at the direction of NE–SW. The pattern of stress permutation results in alternating and interfering strike-slip and normal faulting motions through recent geological times. Such stress permutations are common in brittle tectonics and have been intensively studied in the last few decades (Angelier et al. 1985; Lee et al. 1997; Hu and Angelier 2004; Tranos 2013). The permutation of σ_1 and σ_2 with fairly consistent σ_3 orientation in our study resembles those of extensional tectonic setting in the western United States as described in the study of Angelier et al (1985). The origin of their permutations may relate to several sources that can be caused by actual modifications in the stress field or even little change in tectonic environmental conditions (Hu and Angelier 2004). The extensional deformation with components of normal and strike-slip faulting was also inferred in published studies of the RRF (Allen et al. 1984; Wang et al. 1998; Schoenbohm et al. 2004; Zuchiewicz et al. 2013). The deformation was generally interpreted to have occurred in a transtensional only stress environment. However, under such a stress environment, it is difficult to explain the deformation pattern with a mixture of normal and strike-slip faults and no obvious timing relationship as observed in our study area. Therefore, we propose that the recent tectonic deformations of northern Vietnam may be controlled by an alternating stress environment with a permutation of σ_1/σ_2 and a consistent NE–SW-trending σ_3 instead of a transtensional only stress environment.

Tectonic mechanism for uplift of the Fansipan mountain range

The Fansipan mountain range is located within a complicated tectonic setting where active or potentially active strike-slip faults, such as the DBPF, the RRF, the Da River fault, and the Chay River fault are adjacent to the mountain range. Geophysical observations from a dense broadband seismic array using the teleseismic receiver function analysis (Nguyen et al. 2013) indicated that the crustal layer of this mountainous region is the thickest comparing to that of its surrounding areas in northern Vietnam. Previous study (Zuchiewicz et al. 2013) has inferred that northern Vietnam was dominated by a transtensional stress environment, which only requires a consistent horizontal maximum stress axis (σ_1). However, the results of our study suggest that both the observed strike-slip and normal faults were likely caused by a permutation of σ_1/σ_2 with a consistent σ_3 as discussed in the previous section.

The tectonic mechanism of co-existence of normal and strike-slip faulting is consistent in explaining the differential uplift pattern in the Fansipan mountain range as inferred from the overall analyses of the topographic surface. The SW side of the south part of the mountain range shows elevated topography, steep and short rivers, and high normalized steepness index values, signifying relatively high uplift rates that is spatially associated to the footwall of the Phong Tho-Nam Pia normal faulting. The spatial association between the Phong Tho-Nam Pia Fault and the inferred high uplift rate on the footwall of the fault suggest that normal faulting likely played a role in the uplift of the Fansipan mountain range. On the other sides, the rivers are long and gentle with relative low steepness index values, signifying relatively low uplift rates. Our mapping using the ASTER 30-m DEM imagery shows that the Fansipan mountain range is bounded by the RRF and the DBPF on the NE and NW sides, respectively. Although these two faults are tectonically active, the deformation is dominated by strike-slip movement instead of vertical uplift (Replumaz et al. 2001; Lai et al. 2012; Duong et al. 2013; Tran et al. 2013), that probably was a reason for relatively low uplift rate on these sides of the Fansipan mountain range.

Based on the interpretation from field investigations, DEM data, and river profile analyses, we propose a conceptual tectonic model for the recent movement of the Fansipan mountain range as shown in Fig. 9. The variation in the inferred rock uplift rates along the range is considered as a response to the varying tectonic movements of the fault systems on its different sides. The inferred high uplift rate on the SW side in the south part is suggested to be a result of normal faulting along the Phong Tho-Nam Pia Fault, creating steep and high relief, short and steep rivers, and high normalized steepness index values. On the other side, the movement is dominantly horizontal, resulting in a relatively slow rock uplift rate as compared to the SW side of the south part.

Conclusions

We present a new topographic analysis and stress field data to decipher the tectonic mechanism related to the deformation of the Fansipan mountain range in northern Vietnam. The normal faulting mechanism is proposed to be related to the tectonic uplift of the Fansipan mountain range based on the following observations and analyses: (1) asymmetrical form of topography on the south part of the Fansipan mountain range with short and steep rivers on the SW side; (2) relatively high normalized steepness index values on the SW side of the south part of the range; (3) evidence of

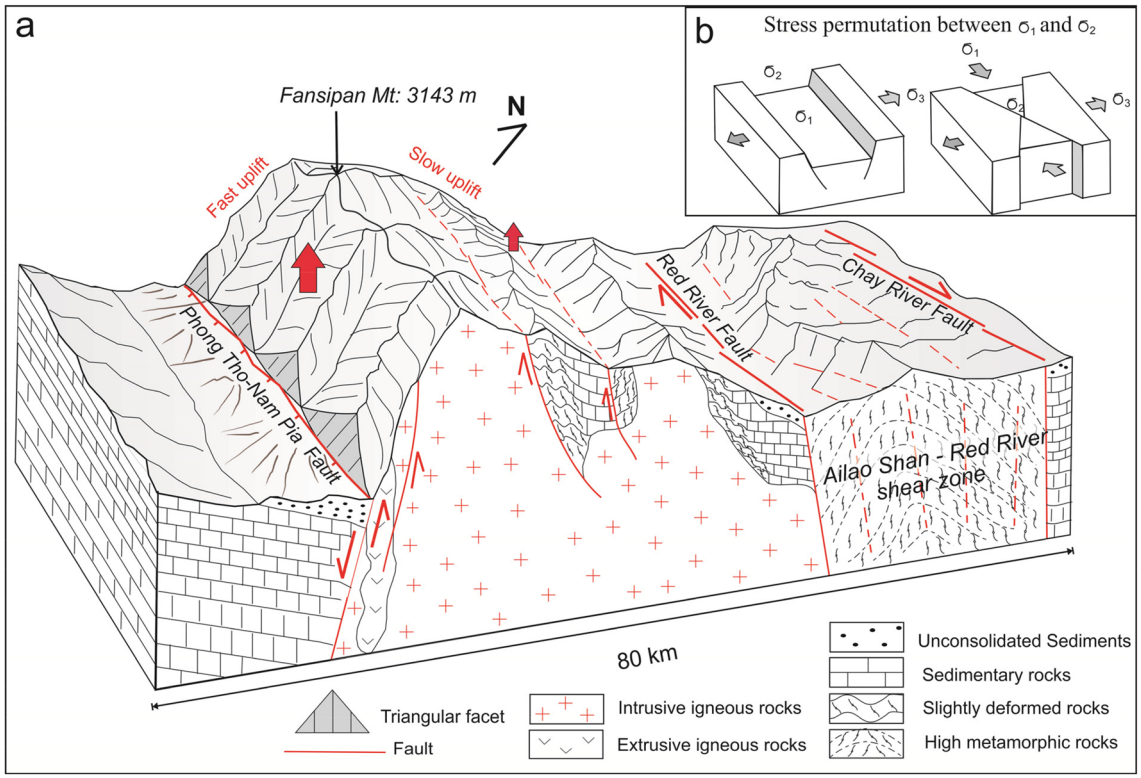

Fig. 9 **a** A conceptual deformation model for the asymmetrical form in the south part of the Fansipan mountain range. The vertical red arrows indicate the relative uplift movement of the Fansipan mountain range. Both the solid and dashed red lines represent faults or inferred faults with the thin arrows indicating direction of movement. This conceptual model is based on the interpretation of topographic observations, river profile analyses, and stress field investigations. The south part of the Fansipan mountain range is bounded by the Phong Tho-Nam Pia fault on the SW side and the Red River fault on the NE side. On the SW side of the mountain, the horizontal extension is accompanied by active normal faulting along the Phong Tho-Nam Pia Fault, which is associated with the relatively high uplift rate on this side of the mountain. On the other side of the mountain, the active strike-slip faults such as the Red River Fault and the Chay River Fault may play a role in the relatively low uplift rate on this side of the mountain. **b** Proposed models for stress permutation of σ_1/σ_2 under the same extensional stress regime of the minimum principal stress (σ_3) that trends at the direction of NE–SW in the Fansipan mountain range

active normal faults along the Phong Tho-Nam Pia fault revealed by field observations and stress analysis. The investigation of fault kinematics at two transects across the Fansipan mountain range shows an inhomogeneous mixture of strike-slip and normal faulting with no obvious timing relationship. The mixture of deformation is interpreted to have occurred in an alternating stress environment with a permutation of σ_1/σ_2 axes and extensional minimum principal stress (σ_3) in the NE–SW direction. Our finding also shows that the deformation pattern is not limited in zones of large strike-slip faults (e.g., the RRF), but distributed across the whole study area. Previous studies have shown that the RRF was experiencing both strike-slip and normal faulting in a transtensional only stress environment. But under such a stress environment, it is difficult to interpret the deformation pattern as observed within the Fansipan mountain range and the surrounding areas. Thus, this study suggests that an alternating stress environment with extensional stress in the NE–SW may dominate recent tectonic deformations of northern Vietnam. Detailed work, such as seismic activities and surface geodesy, may be needed to further constrain most recent deformations in the complex regions of northern Vietnam.

Acknowledgements This research was supported by the Ministry of Science and Technology (MOST) of Taiwan under project numbers 106-2116-M-001-020, 107-2116-M-001-002, 107-2119-M-001-048 and Thematic Project of Academia Sinica (AS-TP-108-M08) to Yu-Chang Chan, as well as MOST108-2628-M-008-002-MY2 to Chih-Tung Chen. We are very grateful for the constructive and helpful comments by Yang Wang and an anonymous reviewer, who have helped improve the focus and presentation of this contribution. We are grateful to Meng-Wan Yeh of National Taiwan Normal University for her comments and support. We would like to thank the Taiwan International Graduate Program and the Institute of Earth Sciences, Academia Sinica, Taiwan for their support.

References

Allen CR, Gillespie AR, Yuan H et al (1984) Red River and associated faults, Yunnan Province, China: auaternary geology, slip rates, and seismic hazard. Geol Soc Am Bull 95:686–700

Angelier J (1979) Determination of the mean principal directions of stresses for a given fault population. Tectonophysics. https://doi.org/10.1016/0040-1951(79)90081-7

Angelier J (1989) From orientation to magnitudes in paleostress determinations using fault slip data. J Struct Geol 11:37–50. https://doi.org/10.1016/0191-8141(89)90034-5

Angelier J (1990) Inversion of field data in fault tectonics to obtain the regional stress-III. A new rapid direct inversion method by analytical means. Geophys J Int 103:363–376. https://doi.org/10.1111/j.1365-246X.1990.tb01777.x

Angelier J, Tarantola A, Valette B, Manoussis S (1982) Inversion of field data in fault tectonics to obtain the regional stress—I. Single phase fault populations: a new method of computing the stress tensor. Geophys J R Astron Soc 69:607–621. https://doi.org/10.1111/j.1365-246X.1982.tb02766.x

Angelier J, Colletta B, Anderson RE (1985) Neogene paleostress changes in the basin and range: a case study at hoover dam. Nevada-Arizona Geol Soc Am Bull 96:347. https://doi.org/10.1130/0016-7606(1985)96<347:NPCITB>2.0.CO;2

Burbank DW, Anderson RS, Robert S (2011) Tectonic geomorphology. Wiley, Hoboken

Chen Z, Burchfiel BC, Liu Y et al (2000) Global Positioning System measurements from eastern Tibet and their implications for India/Eurasia intercontinental deformation. J Geophys Res Solid Earth 105:16215–16227. https://doi.org/10.1029/2000JB900092

Cong Duong C, Yun H-S, Cho J-M (2006) GPS measurements of horizontal deformation across the Lai Chau—Dien Bien (Dien Bien Phu) fault, in Northwest of Vietnam, 2002–2004. Earth Planets Space 58:523–528. https://doi.org/10.1186/BF03351949

Cong DC, Feigl KL (1999) Geodetic measurement of horizontal strain across the Red River fault near Thac Ba, Vietnam, 1963–1994. J Geod 73:298–310. https://doi.org/10.1007/s001900050247

DiBiase RA, Heimsath AM, Whipple KX (2012) Hillslope response to tectonic forcing in threshold landscapes. Earth Surf Process Landforms 37:855–865. https://doi.org/10.1002/esp.3205

Dung PT, Hoa TT, Anh TT et al (2012) New data of Ye Yen Sun granite complex in Phan Si Pan uplift. Vietnam J Earth Sci 34:193–204. https://doi.org/10.15625/0866-7187/34/3/2535

Duong NA, Sagiya T, Kimata F et al (2013) Contemporary horizontal crustal movement estimation for northwestern Vietnam inferred from repeated GPS measurements. Earth Planets Space 65:1399–1410. https://doi.org/10.5047/eps.2013.09.010

Escamilla-Casas JC, Schulz JE (2016) Geofísica internacional. Universidad Nacional Autónoma de México, Instituto de Geofísica, Coyoacán

Faure M, Lepvrier C, Van NV et al (2014) The South China block-Indochina collision: Where, when, and how? J Asian Earth Sci 79:260–274. https://doi.org/10.1016/j.jseaes.2013.09.022

Howard AD, Dietrich WE, Seidl MA (1994) Modeling fluvial erosion on regional to continental scales. J Geophys Res Solid Earth 99:13971–13986. https://doi.org/10.1029/94JB00744

Hu J-C, Angelier J (2004) Stress permutations: three-dimensional distinct element analysis accounts for a common phenomenon in brittle tectonics. J Geophys Res Solid Earth. https://doi.org/10.1029/2003JB002616

King RW, Shen F, Clark Burchfiel B et al (1997) Geodetic measurement of crustal motion in southwest China. Geology 25:179. https://doi.org/10.1130/0091-7613(1997)025<0179:GMOCMI>2.3.CO;2

Kirby E, Ouimet W (2011) Tectonic geomorphology along the eastern margin of Tibet: insights into the pattern and processes of active deformation adjacent to the Sichuan Basin. Geol Soc Lond Spec Publ 353:165–188. https://doi.org/10.1144/SP353.9

Kirby E, Whipple K (2001) Quantifying differential rock-uplift rates via stream profile analysis. Geology 29:415. https://doi.org/10.1130/0091-7613(2001)029<0415:QDRURV>2.0.CO;2

Kirby E, Whipple KX (2012) Expression of active tectonics in erosional landscapes. J Struct Geol 44:54–75

Lai KY, Chen YG, Lâm D (2012) Pliocene-to-present morphotectonics of the Dien Bien Phu fault in northwest Vietnam. Geomorphology 173–174:52–68. https://doi.org/10.1016/j.geomorph.2012.05.026

Lan C-Y, Chung S-L, Lo C-H et al (2001) First evidence for Archean continental crust in northern Vietnam and its implications for crustal and tectonic evolution in Southeast Asia. Geology 29:219. https://doi.org/10.1130/0091-7613(2001)029<0219:FEFACC>2.0.CO;2

Lee J-C, Angelier J, Chu H-T (1997) Polyphase history and kinematics of a complex major fault zone in the northern Taiwan mountain belt: the Lishan Fault. Tectonophysics 274:97–115. https://doi.org/10.1016/S0040-1951(96)00300-9

Leeder MR, Jackson JA (1993) The interaction between normal faulting and drainage in active extensional basins, with examples from the western United States and central Greece. Basin Res 5:79–102. https://doi.org/10.1111/j.1365-2117.1993.tb00059.x

Leloup PH, Kienast J-R (1993) High-temperature metamorphism in a major strike-slip shear zone: the Ailao Shan—Red River, People's Republic of China. Earth Planet Sci Lett 118:213–234. https://doi.org/10.1016/0012-821X(93)90169-A

Leloup PH, Arnaud N, Lacassin R et al (2001) New constraints on the structure, thermochronology, and timing of the Ailao Shan-Red River shear zone, SE Asia. J Geophys Res Solid Earth 106:6683–6732. https://doi.org/10.1029/2000JB900322

Leloup PH, Tapponnier P, Lacassin R, Searle MP (2007) Discussion on the role of the Red River shear zone, Yunnan and Vietnam, in the continental extrusion of SE Asia Journal, Vol. 163, 2006, 1025–1036. J Geol Soc London 164:1253–1260. https://doi.org/10.1144/0016-76492007-065

Minh LH, Masson R, Bourdillon A et al (2014) Recent crustal motion in Vietnam and in the Southeast Asia region by continuous GPS data. Vietnam J Earth Sci 36:1–13. https://doi.org/10.15625/0866-7187/36/1/4132

Molnar P, Tapponnier P (1975) Cenozoic Tectonics of Asia: effects of a continental collision: features of recent continental tectonics in Asia can be interpreted as results of the India-Eurasia collision. Science 80–(189):419–426. https://doi.org/10.1126/science.189.4201.419

Mukherjee S, Joshi PK, Mukherjee S et al (2012) Evaluation of vertical accuracy of open source Digital Elevation Model (DEM). Int J Appl Earth Obs Geoinf 21:205–217. https://doi.org/10.1016/j.jag.2012.09.004

Nam TN (2001) Ages of the Ca Vinh and Xom Giau complexes: first reliable evidence from SHRIMP U-Pb zircon dating. Geol Ser A 262:1–11

Nguyen V-D, Huang B-S, Le T-S et al (2013) Constraints on the crustal structure of northern Vietnam based on analysis of teleseismic converted waves. Tectonophysics 601:87–97. https://doi.org/10.1016/J.TECTO.2013.04.031

Niemann JD, Gasparini NM, Tucker GE, Bras RL (2001) A quantitative evaluation of playfair's law and its use in testing long-term stream erosion models. Earth Surf Process Landforms 26:1317–1332. https://doi.org/10.1002/esp.272

Replumaz A, Lacassin R, Tapponnier P, Leloup PH (2001) Large river offsets and Plio-Quaternary dextral slip rate on the Red River fault (Yunnan, China). J Geophys Res Solid Earth 106:819–836

Santillan JR, Makinano-Santillan M (2016) Vertical accuracy assessment of 30-m resolution ALOS, ASTER, and SRTM global DEMS over Northeastern Mindanao, Philippines. Int Arch Photogramm Remote Sens Spat Inf Sci - ISPRS Arch 41:149–156. https://doi.org/10.5194/isprsarchives-XLI-B4-149-2016

Schmidt-Thomé P, Nguyen TH, Pham TL et al (2015) Climate change adaptation measures in Vietnam. Springer International Publishing, Cham

Schoenbohm LM, Whipple KX, Burchfiel BC, Chen L (2004) Geomorphic constraints on surface uplift, exhumation, and plateau growth in the Red River region, Yunnan Province, China. Bull Geol Soc Am 116:895–909. https://doi.org/10.1130/B25364.1

Shen Z-K, Lü J, Wang M, Bürgmann R (2005) Contemporary crustal deformation around the southeast borderland of the Tibetan Plateau. J Geophys Res Solid Earth. https://doi.org/10.1029/2004JB003421

Shu L, Faure M, Wang B et al (2008) Late Palaeozoic-Early Mesozoic geological features of South China: response to the Indosinian collision events in Southeast Asia. Comptes Rendus Geosci 340:151–165. https://doi.org/10.1016/J.CRTE.2007.10.010

Snyder NP, Whipple KX, Tucker GE, Merritts DJ (2000) Landscape response to tectonic forcing: digital elevation model analysis of stream profiles in the Mendocino triple junction region, northern California. Geol Soc Am Bull 112:1250–1263. https://doi.org/10.1130/0016-7606(2000)112<1250:LRTTFD>2.0.CO;2

Tapponnier P, Peltzer G, Le Dain AY et al (1982) Propagating extrusion tectonics in Asia: new insights from simple experiments with plasticine. Geology 10:611–616. https://doi.org/10.1130/0091-7613(1982)10<611:PETIAN>2.0.CO;2

Tapponnier P, Peltzer G, Armijo R (1986) On the mechanics of the collision between India and Asia. Geol Soc Lond Spec Publ 19:113–157. https://doi.org/10.1144/GSL.SP.1986.019.01.07

Tapponnier P, Lacassin R, Leloup PH et al (1990) The Ailao Shan/Red River metamorphic belt: tertiary left-lateral shear between Indochina and South China. Nature 343:431–437. https://doi.org/10.1038/343431a0

Tran DT, Nguyen TY, Duong CCô, et al (2013) Recent crustal movements of northern Vietnam from GPS data. J Geodyn 69:5–10. https://doi.org/10.1016/j.jog.2012.02.009

Tran TH, Lan C-Y, Usuki T et al (2015) Petrogenesis of Late Permian silicic rocks of Tu Le basin and Phan Si Pan uplift (NW Vietnam) and their association with the Emeishan large igneous province. J Asian Earth Sci 109:1–19. https://doi.org/10.1016/J.JSEAES.2015.05.009

Tranos MD (2013) The TR method: the use of slip preference to separate heterogeneous fault-slip data in compressional stress regimes. The surface rupture of the 1999 Chi-Chi Taiwan earthquake as a case study. Tectonophysics 608:622–641. https://doi.org/10.1016/j.tecto.2013.08.017

Usuki T, Lan C-Y, Tran TH et al (2015) Zircon U-Pb ages and Hf isotopic compositions of alkaline silicic magmatic rocks in the Phan Si Pan-Tu Le region, northern Vietnam: identification of a displaced western extension of the Emeishan Large Igneous Province. J Asian Earth Sci 97:102–124. https://doi.org/10.1016/J.JSEAES.2014.10.016

Vu TM, Raghavan SV, Liong SY, Mishra AK (2018) Uncertainties of gridded precipitation observations in characterizing spatio-temporal drought and wetness over Vietnam. Int J Climatol 38:2067–2081. https://doi.org/10.1002/joc.5317

Wang E, Burchfiel BC, Royden LH et al (1998) Late Cenozoic Xianshuihe-Xiaojiang, Red River, and Dali fault systems of Southwestern Sichuan and Central Yunnan, China. Spec Pap Geol Soc Am 327:1–108. https://doi.org/10.1130/0-8137-2327-2.1

Whipple KX (2004) Bedrock rivers and the geomorphology of active orogens. Annu Rev Earth Planet Sci 32:151–185. https://doi.org/10.1146/annurev.earth.32.101802.120356

Whipple KX, Tucker GE (1999) Dynamics of the stream-power river incision model: implications for height limits of mountain ranges, landscape response timescales, and research needs. J Geophys Res Solid Earth 104:17661–17674. https://doi.org/10.1029/1999JB900120

Whipple K, Wobus C, Crosby B et al (2007) New tools for quantitative geomorphology: extraction and interpretation of stream profiles from digital topographic data. GSA short course, p 506

Wobus C, Whipple KX, Kirby E et al (2006) Tectonics from topography: Procedures, promise, and pitfalls. In: Special Paper 398: Tectonics, Climate, and Landscape Evolution. Geological Society of America, pp 55–74

Zhang RY, Lo CH, Chung SL et al (2013) Origin and Tectonic implication of Ophiolite and Eclogite in the Song Ma Suture Zone between the South China and Indochina Blocks. J Metamorph Geol 31:49–62. https://doi.org/10.1111/jmg.12012

Zhou M-F, Chen WT, Wang CY et al (2013) Two stages of immiscible liquid separation in the formation of Panzhihua-type Fe-Ti-V oxide deposits, SW China. Geosci Front 4:481–502. https://doi.org/10.1016/J.GSF.2013.04.006

Zuchiewicz W, Cu'ò'ng NQ, Zasadni J, Yêm NT, (2013) Late Cenozoic tectonics of the Red River Fault Zone, Vietnam, in the light of geomorphic studies. J Geodyn 69:11–30. https://doi.org/10.1016/j.jog.2011.10.008